Cellulose (2010) 17:559–574
DOI 10.1007/s10570-009-9393-y

Oxygen and oil barrier properties of microfibrillated cellulose films and coatings

Christian Aulin · Mikael Gällstedt · Tom Lindström

Received: 5 October 2009 / Accepted: 14 December 2009 / Published online: 10 January 2010

Abstract The preparation of carboxymethylated microfibrillated cellulose (MFC) films by dispersion-casting from aqueous dispersions and by surface coating on base papers is described. The oxygen permeability of MFC films were studied at different relative humidity (RH). At low RH (0%), the MFC films showed very low oxygen permeability as compared with films prepared from plasticized starch, whey protein and arabinoxylan and values in the same range as that of conventional synthetic films, e.g., ethylene vinyl alcohol. At higher RH's, the oxygen permeability increased exponentially, presumably due to the plasticizing and swelling of the carboxymethylated nanofibers by water molecules. The effect of moisture on the barrier and mechanical properties of the films was further studied using water vapor sorption isotherms and by humidity scans in dynamic mechanical analysis. The influences of the degree of nanofibrillation/dispersion on the microstructure and optical properties of the films were evaluated by field-emission scanning electron microscopy (FE-SEM) and light transmittance measurements, respectively. FE-SEM micrographs showed that the MFC films consisted of randomly assembled nanofibers with a thickness of 5–10 nm, although some larger aggregates were also formed. The use of MFC as surface coating on various base papers considerably reduced the air permeability. Environmental scanning electron microscopy (E-SEM) micrographs indicated that the MFC layer reduced sheet porosity, i.e., the dense structure formed by the nanofibers resulted in superior oil barrier properties.

Keywords MFC · Barrier · Oil · Oxygen permeability · Nanofibers · Nanocellulose · Packaging · Films · SEM · Coating

Electronic supplementary material The online version of this article (doi:10.1007/s10570-009-9393-y) contains supplementary material, which is available to authorized users.

C. Aulin (✉)
BIM Kemi AB, Box 3102, 443 03 Stenkullen, Sweden
e-mail: caulin@polymer.kth.se

C. Aulin
Department of Fibre and Polymer Technology, School of Chemical Science and Engineering, The Royal Institute of Technology, 100 44 Stockholm, Sweden

M. Gällstedt · T. Lindström
Innventia AB, Box 5604, 114 86 Stockholm, Sweden

Introduction

Depending upon the application, low oxygen permeability (OP) as well as mechanical strength and flexibility can be important target properties for packaging films laminates and/or coatings. The great majority of plastic materials in use today are based on fossilic raw materials. Sustainable development in the future is expected to increase the use of renewable materials. Reviews on biodegradable coatings and

films are available elsewhere (McHugh and Krochta 1994a, b, c; Arvanitoyannis et al. 1997; Avranitoyannis et al. 1997; Miller and Krochta 1997; Psomiadou et al. 1997; Arvanitoyannis et al. 1998; Arvanitoyannis 2006; Hartman et al. 2006a, b; Krochta 2007; Hansen and Plackett 2008).

In recent years, there has also been an increasing interest in oil-resistant papers and paperboards in new products. This demand is attributed to the continuously growing packaging markets for food such as bakery products, pet foods and fast foods (Deisenroth et al. 1998).

The use and environment-friendliness of fluorochemicals for oil-resistant paper have been heavily debated during recent years due to their toxicity and low rate of biodegradation (Kissa 2001). Hence, the development of new additives that impart oil resistance is an interesting research area in combination with studies of the fundamental processes that control the spreading and absorption of oils.

A renewable biomaterial that may be an alternative for oil and gas barrier applications is microfibrillated cellulose (MFC). The term "microfibrillated cellulose" (MFC) refers to cellulosic fibrils disintegrated from the plant cell walls. The preparation of MFC from wood was first explored by Turbak et al. (Turbak et al. 1983) and Herrick et al. (1983) more than two decades ago. Through a homogenization process, wood pulp is disintegrated to give a material where the fibres are degraded and opened-up into their sub-structural elementary fibrils and microfibrils. After homogenization, the final fibrillar elements have a width lower than 20 nm and a length of up to several μm, which is the microfibrillar size in wood cellulosic fibers (Bardage et al. 2004). In this context, the term microfibril refers to an elementary fibril aggregate, which is a distinct sub-structural unit in wood cellulosic fibers (Fengel 1971).

The partly crystalline microfibrils (Aulin et al. 2009) in combination with the ability of the dried films to form a dense network held together by strong inter/intra-fibrillar bonds, suggest that these films should potentially have barrier properties and be an interesting alternative to, for example, plastics. Due to the rather high degree of crystallinity of MFC (63 ± 8.6%; Aulin et al. 2009), the permeability of MFC is expected to be limited, but, gas diffusion may nevertheless occur through the voids in the microfibril network. Indeed, Fukuzumi et al. (2009) have investigated the OP of cellulose nanofibers prepared by 2,2,6,6-tetramethylpiperdine-1-oxyl radical (TEMPO)-mediated oxidation and have found such films to be good barriers under dry conditions. Similar studied were made by Syverud et al. who report promising air barriers of MFC-coated papersheets (Syverud and Stenius 2009).

The aim of this study was to evaluate MFC for potential application in packaging materials and bioplastics. MFC films were prepared and thoroughly characterized in terms of their morphology and OP. Two papers with different air permeances were coated with MFC to study the conditions required to obtain a packaging material with a good oil barrier. MFC may be a promising barrier material, but, there is a need to further study the fundamental properties of MFC films and coatings such as permeability, moisture-sensitivity and mechanical properties.

Experimental section

Materials

In the manufacture of MFC, a commercial sulfite softwood-dissolving pulp (Domsjö Dissolving Plus; Domsjö Fabriker AB, Domsjö, Sweden), from 60% Norwegian spruce (Piceaabies) and 40% Scottish Pine (Pinus sylvestris), with a hemicellulose content of 4.5% and a lignin content of 0.6% was used. The pulp was thoroughly washed with deionized water and used in its never-dried form. The anionic MFC used in this study was prepared in a manner similar to a previously described procedure (Pääkkö et al. 2007) but using a carboxymethylation (Wågberg et al. 2008) pretreatment instead of an enzymatic pretreatment of the fibers. In brief, the dissolving pulp (Domsjö dissolving plus) was first dispersed in deionized water at 10,000 revolutions in an ordinary laboratory reslusher. The fibers were than solvent-exchanged to ethanol by washing the fibers in ethanol four times with an intermediate filtration step. The fibers were then impregnated for 30 min with a solution of 10 g of monochloroacetic acid in 500 mL of isopropanol. This carboxymethylation reaction was allowed to continue for 1 h. Following the carboxymethylation step, the fibers were filtered and washed in three steps: first with deionized water, then with 0.1 M acetic acid, and finally with deionized water. The fibers were then impregnated with a $NaHCO_3$

solution (4 wt% solution) in order to convert the carboxyl groups to their sodium form. Finally, the fibers were washed with deionized water and drained on a Büchner funnel.

After this treatment, the fibers were homogenized using a high-pressure fluidizer (Microfluidizer M-110EH, Mircofluidics Corp). Homogenization was made at a starting fiber consistency of 2 wt% and an operating pressure of 1,650 bar. A total of 10 passes through the homogenizator were carried out, each with subsequent dilution step, to obtain a highly fibrillated 0.13 wt% MFC dispersion, optimal for film preparation. A total of 6 passes, each with a subsequent dilution step, were carried out for a 0.85 wt% MFC dispersion used for the paper-coating process.

Series of 1, 2, 4 and 5 passes through the homogenizator equipment were made to study the effect of nanofibrillation/degree of dispersion of MFC on the OP and optical properties of the films prepared. The final concentrations of the MFC dispersions that were treated 1, 2, 4 or 5 times in the homogenizator equipment were 2, 1.06, 1.15 and 1.13 wt%, respectively.

The total and surface charge densities of the highly carboxymethylated MFC dispersions were found to be ca. 515 (Wågberg et al. 2008) and 426 μeq./g using conductometric (Wågberg et al. 1987) and polyelectrolyte titration (Winter et al. 1986), respectively.

Dynamic Rheology

Dynamic shear experiments were carried out using a plate-and-plate geometry (plate diameter 60 mm and plate-to-plate gap 1 mm) on a stress-controlled Bohlin Gemini rheometer Model 150 (Malvern Instruments Ltd, UK) equipped with a temperature-control system. The MFC dispersions were directly introduced onto the plate after the preparation.

Preparation of films

The MFC dispersions (Na-form) were poured onto polystyrene Petri dishes with a diameter of 14 cm, and films were allowed to form upon drying at a temperature of 23 °C and a relative humidity (RH) of 50%. The dried free-standing films were stored in these conditions until analysis.

Density/thickness/surface roughness measurements

The thickness and the RMS roughness of the MFC films were determined using a white-light interferometric profilometer with a lateral and z-resolution of 1.1 μm and 1 nm, respectively (NewView 5010, Zygo Corporation, USA). The technique is based on reflection of white light from the sample surface, which then interferes with light reflected from an internal reference surface. Images over the sample are collected with a CCD camera scanning the object in the height (z) direction. The resulting interference images were analyzed in the frequency domain giving a high-resolution three-dimensional image (height map) of the film topography. To evaluate the MFC film thickness, topographical images (713 × 535 μm) were taken to include the edge of the film, i.e., the transition from the MFC film coated on the polystyrene Petri dish to the pure polystyrene Petri dish. The RMS surface roughness was determined from a surface area of 177 × 133 μm. The thickness values are reported as averages of three film measurements using height steps from cross sections within the image areas. The density of the films was obtained by dividing the grammage (g/m^2) by the thickness of the films.

Oxygen permeability

The oxygen transmission rate (OTR) tests were performed with a Mocon Ox-Tran Model 2/20 apparatus (Mocon, Minneapolis, USA) in accordance with ASTM D 3985-95 and the test conditions were 23 °C at 0, 20, 40, 50, 60, 70 and 80% RH. The sample area was 5 or 50 cm^2 and the partial pressure of the oxygen was 1 atm. The OTR was normalized with respect to the oxygen pressure, sample area and material thickness to yield the OP.

Dynamic mechanical analysis

The mechanical behavior of the films was studied in tension at a temperature of 30 °C using a Perkin Elmer dynamic mechanical analyser (DMA). The width of the sample was 3–3.5 mm and the clamping distance was 9–12 mm. The storage modulus was measured continuously with a dynamic load giving

the deformation amplitude of 3 μm, and a static load of 200% of the dynamic load.

Tests were made at different surrounding relative humidity, and the atmosphere around the samples was controlled by a WETSYS humidity generator. The program was initiated at 5% RH, followed by a ramp of 0.5% RH per min until 90% RH was reached. In order to release built-in drying tensions in the film a pre-scan at a speed of 1% RH per min was made followed by drying for 2 h before the actual humidity scan.

Water vapor sorption isotherm

The water vapour sorption isotherms were made at 30 °C using a dynamic water vapour sorption (DWS) equipment from Surface Measurements Systems, UK. The relative humidity was changed in ten equal steps, from 0 to 95%.

Optical properties

The regular light transmittances of the films were measured at wavelengths from 200 to 800 nm using an ultraviolet (UV)-visible spectrometer (Cary 1E, Varian Inc., USA). The transmittance was measured by placing the specimens vertically in special sample holders 5 cm from the light source.

Scanning electron microscopy

For the micro-structural analysis of the MFC films, the specimens were studied with a Hitachi S-4800 field emission scanning electron microscope (FE-SEM; Spectral Solution, Sweden) to obtain secondary electron images. The specimens were fixed on a metal stub with colloidal graphite paint and coated with a 6 nm thick gold/palladium layer using a Cressington 208 h high resolution sputter coater. The accelerating voltage was 1 kV and working distance was about 4 mm.

To analyze the surface texture of the coated and uncoated papers, an electron microscope Philips XL30 ESEM-FEG (environmental scanning electron microscope-field emission gun) was used. The surfaces of the paper samples were coated with a thin conducting layer of gold and imaged in the high vacuum mode using a SE detector (secondary electrons). The accelerating voltage was 5 kV and working distance was about 7 mm.

Paper coating

A kraft paper (wrapping paper) and a greaseproof paper with different air permeability levels were used as base paper for the coatings. The papers were made from softwood pulp and produced by Nordic Paper AB, Säffle, Sweden. The kraft paper was unbleached and was not pigment-filled. The compositions of the base papers and their air permeability-values are found in Table 1.

The base papers were coated on a bench scale with an aqueous MFC dispersion (Na-form) having a concentration of 0.85 wt%, using a rod coater for sheets, K101 Control Coater, RK Print Coat Instruments Ltd, Herts, UK. Six coat weights were applied, where the coat weight was varied by varying the diameter of the wire on the rod. The sheets were coated on one side and were dried under ambient conditions. Immediately before the coating procedure, the MFC was mechanically stirred at a shear rate of 700/s using a four-blade propeller stirrer (RW 20, IKA, Germany).

The properties of the coated papers were investigated without any calendering. The papers were stored at 23 °C and 50% RH for at least 3 days before testing.

In general, the coat weight (g/m^2) of MFC applied in this study was rather low, which makes it difficult to obtain a precise value from gravimetric measurements. Nevertheless, the coat weight of MFC was indirectly determined by analyzing the amount of Na^+ in the coated papers using an atomic absorption spectrometer (AAS; Perkin-Elmer AAnalyst 300, US). Before the flame absorption, small amounts of coated papers were dissolved in 15 mL concentrated HNO_3 and thereafter treated in a laboratory microwave System (MARS, Modell 907510, CEM Corporation, US) at 180 °C and 600 Psi. Three atomic absorption measurements were made for each paper. The coat weight MFC was calculated under the assumption that the total charge density of MFC was 515 μekv./g. (Wågberg et al. 2008).

Table 1 Compositions of commerical base papers used for coating

	Furnish	Air permeability (nm/Pa s)
Kraft (wrapping)	Unbleached sulphate	69,000
Greaseproof	Bleached sulphate	660

Air permeability

The air permeance tests were performed using an Air Permeance Tester SE166 (Lorentzen & Wettre AB, Sweden) in accordance with SCAN P-26:78 (Scandinavian Pulp, Paper and Board Testing Committee, standardized test-method jointly for the pulp and paper industry in Finland, Norway and Sweden, www.nordstand.com). The results are reported as the average of four measurements.

Oil resistant testing

The oil resistance was measured in accordance with Tappi T-454, the turpentine oil [(γ_{lv} = 24.2 mN/m (Asthana et al. 1964); Sigma–Aldrich, purified, Germany] being applied on the coated side. In addition to the Tappi T-454 tests, the penetration time of castor oil [γ_{lv} = 35.8 mN/m (Schwartz 1981); Fluka, purum, Germany] was also studied. The results are reported as the average of three measurements. The viscosity of turpentine and castor oil was measured to 0.002 and 0.5 Pas, respectively, (shear rate 100/s) at 25 °C using a Bohlin Gemini rheometer Model 150 (Malvern Instruments Ltd, UK).

Results

MFC dispersion viscosities

The shear viscosities of the MFC dispersions (1 wt%) are shown as a function of shear rate in Fig. 1. The suspensions show a large decrease in viscosity with increasing shear rate, i.e., they are shear thinning. The shear thinning of MFC was early recognized in the literature for the materials prepared solely by mechanical disintegration (Herrick et al. 1983). Therefore, an MFC gel can be considered as a paste material (Kendall 2001) or pseudoplastic material (Pääkkö et al. 2007). This behavior is also a characteristic of cellulose nano-whiskers (Orts et al. 1998; Ebeling et al. 1999; Bercea and Navard 2000) or microcrystalline cellulose hydrogels (Ono et al. 1998). On exposure to an increasing shear rate, the network falls apart and individual elements start to flow. It is also clear in Fig. 1, that the viscosity of the samples increase with number of passes through the homogenization equipment, i.e., with increasing

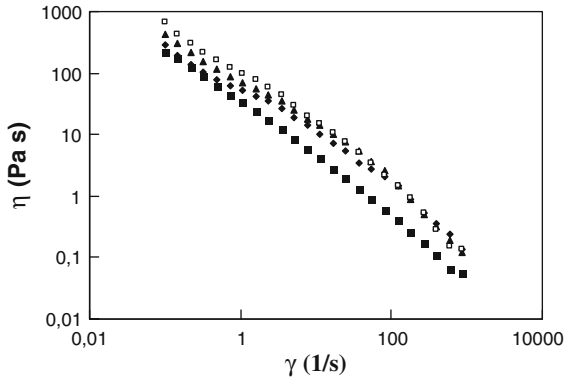

Fig. 1 Influence of shear rate on the viscosity of different degree of fibrillation; (*filled square* = 1 wt%, 1 pass), (*filled diamond* = 1 wt%, 2 passes), (*filled triangle* = 1 wt%, 4 passes) and (*open square* = 1 wt%, 5 passes)

fibrillation of the nanofibers. This is probably a result of an increased swelling capacity and increased water uptake due to more exposed surface areas of the carboxymethylated nanofibrils.

Structure of the films

Figure 2a and b shows two films prepared from MFC dispersions homogenized once and ten times, respectively. Figure 2 shows a direct comparison at a magnification of 30,000×. The random orientation and distribution of the nanofibers is apparent. Direct measurements of the width of the microfibrils in these images show values of about 5–10 nm, although some larger fibrous entities or cell wall fragments are present, especially in the MFC film prepared from a dispersion homogenized once (Fig. 2b), which also exhibits a slightly broader fibril size distribution and a rougher film characteristic as indicated by the FE-SEM images (see SEM images in Supporting Information, S1 and S2). The figures provide a good illustration of the cellulose nanofiber network and they indicate that some porosity can be suspected. The RMS surface roughness, as determined by the white-light interferometric profilometer, was found to be 75 ± 34 nm and 1,478 ± 885 nm for the MFC films prepared from dispersions homogenized ten times and once, respectively. The density of crystalline cellulose has been determined recently, using the most recent cellulose Iβ crystal structure, to 1.63 g/cm^3 (Diddens et al. 2008; Chanzy 2009). The density of amorphous cellulose is generally given as

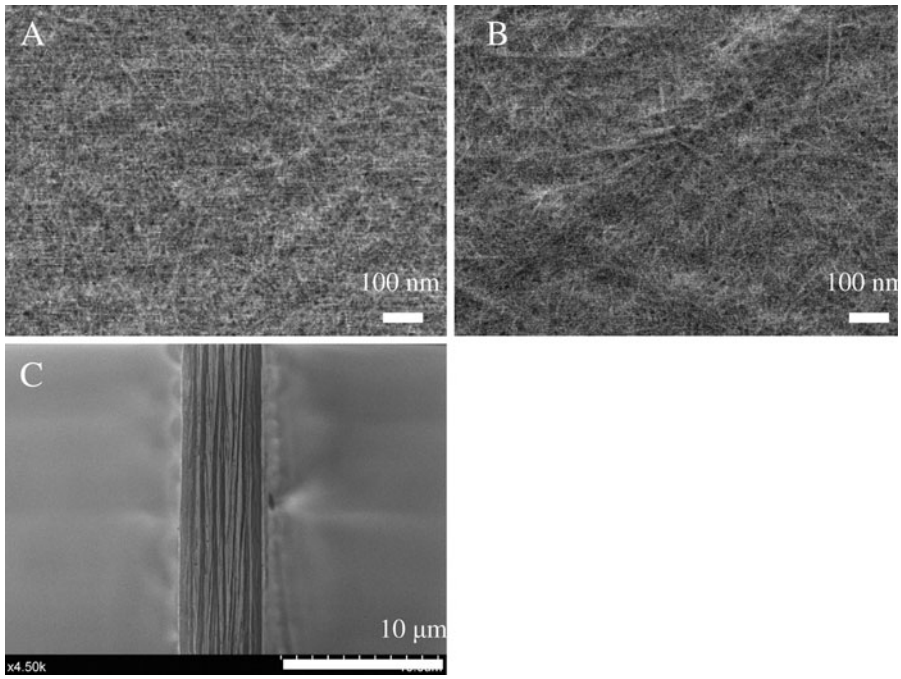

Fig. 2 High-magnification (**a**, **b** 30,000× and **c** 4,500×) FE-SEM images of MFC films prepared from dispersions homogenized (**a**) 10 times and (**b**) once, respectively. The scale bars are 100 nm. **c** Micrograph of a cross-section view of a MFC film (thickness 5.1 µm). The *scale bar* is 10 µm

1.48 g/cm^3.(Chen et al. 2004) Since the crystallinity of the MFC films is substantially less than 100% (ca. 63%), (Aulin et al. 2009) the density of MFC films is expected to be between 1.48 and 1.63 g/cm^3. Indeed, the density of the films was determined to be 1.57 ± 0.03 g/cm^3, indicating a low porosity.

Figure 2c shows a cross-section of a typical free-standing film (grammage 8 g/m^2). The micrograph indicates a lamellar organization of the MFC. The thickness of the film is ca. 5.1 µm as measured by the FE-SEM software. A lamellar structure of MFC films has also been reported earlier in the literature (Svagan et al. 2007; Henriksson et al. 2008).

Optical properties

In previous studies, it has been shown that the light transmittance of composites prepared with fibrillated pulp and acrylic resin increases with increasing degree of fibrillation (Yano et al. 2005). Hence, the light transmittance of the MFC films was evaluated at wavelengths between 200 and 800 nm as an indirect estimate of the fiber width distribution. The light transmittance of two MFC films (grammage 8 g/m^2, thickness 5.1 µm) prepared from MFC dispersions homogenized once and 10 times, respectively is shown versus wavelength in Fig. 3. The transmittance at 600 nm was about 90% for the film homogenized 10 times and was about 25% for the film homogenized once. The MFC film prepared from a dispersion homogenized 10 times was transparent compared with the film prepared from a dispersion homogenized once that appeared opaque (photograph, Fig. 3).

Oxygen barrier properties

Oxygen transmission rates of the MFC films are plotted as a function of film grammage (g/m^2; Fig. 4a) and % RH (Fig. 4b). The OTR decreased with increasing film grammage. As expected, the grammage (or thickness) of the films is an important factor governing the OTR of the material. MFC films have a potential for use in barrier application, although water sorption and high relative humidity can be problematic. The OTR of two films with grammages of 5 and 8 g/m^2 was therefore determined at different RH's. When the RH was increased from 0 to 80%, the OTR increased dramatically (Fig. 4b). At a RH higher than

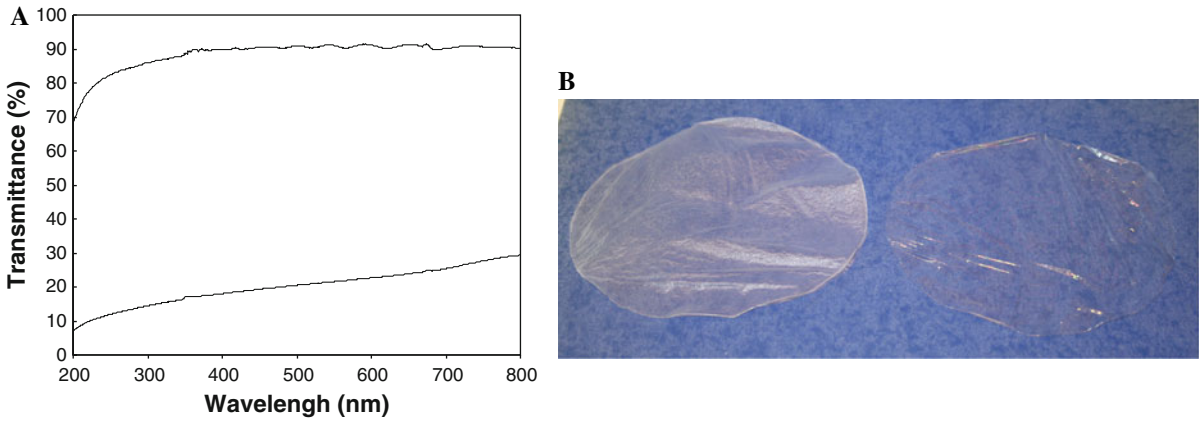

Fig. 3 UV-vis transmittance spectrum and a photograph showing the appearance of MFC films prepared from dispersions homogenized (**a**) once and (**b**) 10 times, respectively. The thicknesses of the films are 5.1 μm

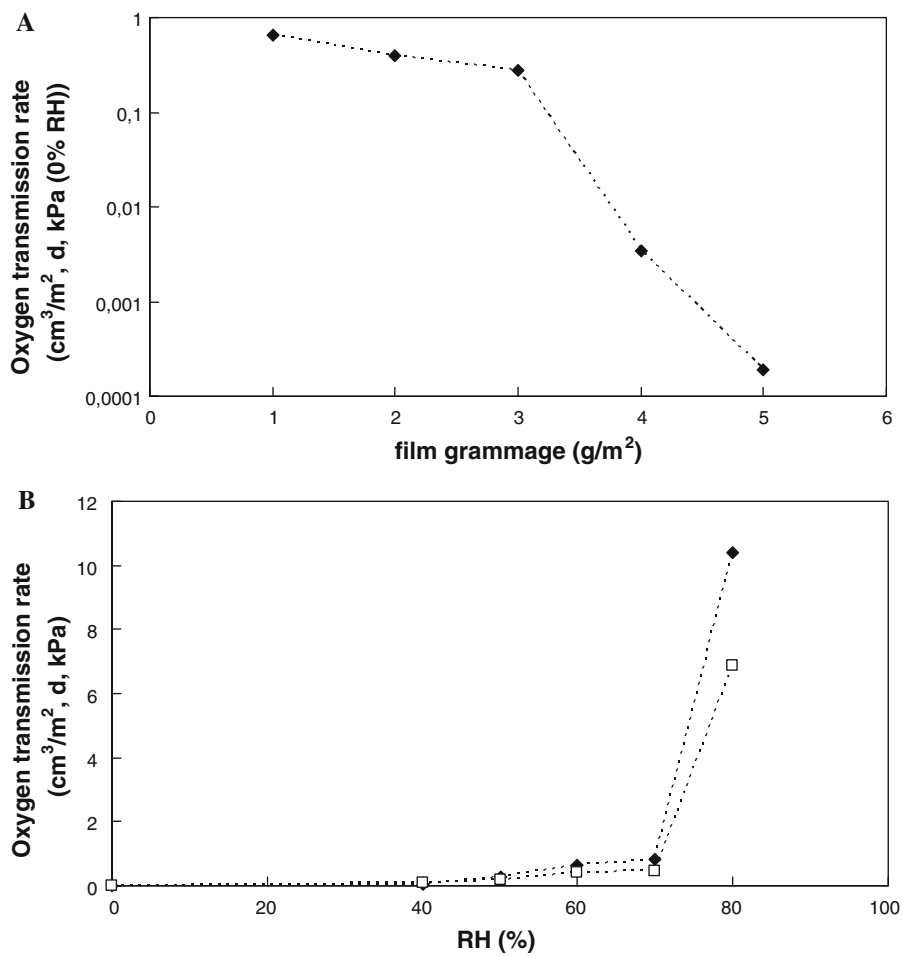

Fig. 4 **a** Effect of MFC film grammage (g/m^2) on oxygen transmission rate (OTR) **b** Effect of relative humidity (% RH) on oxygen transmission rate (OTR) of MFC films with grammages of 5 (*filled diamond*) and 8 (*open square*) g/m^2

70%, there was a sharp increase in permeability. The influence of film thickness on the OP was also studied. Interestingly, the OPs were founded to be 0.009 and 0.0006 cm^3 μm/ (m^2 day kPa) for film thicknesses of 2.54 and 3.19 μm, respectively. The OP of 5 g/m^2 grammage films was measured as a function of the

number of passes through the homogenizator, i.e., the degree of nanofibrillation. Despite an increase in the number of passes during the preparation of the films, the OTR were found to be very similar.

Effect of water

It is well-known that the properties of polysaccharides such as cellulose are affected by water. The hydrophilicity depends on the fiber type and preparation and can be considerably influenced by surface modifications such as carboxymethylation. To examine the effect of the surrounding humidity on the water content of MFC, a water vapor sorption isotherm was measured as shown in Fig. 5. Two measurements were made and the variations were small. The shape of the curve for MFC is characteristic of systems with strong polymer–polymer and polymer–solvent interactions (type II isotherm; Kohler et al. 2006). The MFC displayed an accelerating water uptake above 80% RH and due to partial replacement of MFC–MFC hydrogen bonds with MFC–water hydrogen bonds. The shape of the curve matches previously reported water vapor sorption isotherms of cellulose I, (Kohler et al. 2006) although the absolute water content values at different %RH are higher, presumably due to the carboxyl content.

Humidity scans in DMA show how the modulus of a MFC film prepared from a dispersion homogenized ten times depends on the atmosphere humidity. With increasing RH, the storage modulus decreases from approximately 30–18.9 GPa at 5 and 90% RH, respectively (Fig. 6). Water present in the amorphous segments acts as a plasticizer, reducing the intermolecular interactions between the MFC fibrils, thus reducing the stiffness of the material. Tan δ, i.e. the loss modulus divided by the storage modulus, was measured to be constant below 0.1 and independent towards changes in RH. This indicates that the mechanical behavior of the films in tension was dictated by the elastic component. The intrinsic elastic modulus of cellulose fibers depends on the degree of crystallinity. In particular, the highest elastic modulus measured for a crystalline cellulose fiber is $E_C = 220$ GPa (Diddens et al. 2008). It is clear that the modulus of the MFC film at 0% RH (30 GPa) is much smaller than for the highly oriented crystalline cellulose fibers, and this could be due to its comparatively lower degree of crystallinity (Aulin et al. 2009; ca. 63%) and random orientation of the microfibril network. Analysis by Cox et al. (Cox 1952) have been used to relate the modulus of a highly oriented polymeric fiber (E) to the modulus of randomly oriented fibers in network or film by the following equation:

$$E = 3 * E_{\text{film}} \tag{1}$$

and the modulus of a highly oriented polymeric fiber (E) to the crystal (E_C) and amorphous modulus (E_A) by the relationship:

$$\frac{1}{E} = \frac{v_1}{E_C} + \frac{v_2}{E_A} \tag{2}$$

where v_1 and v_2 are the volume fractions of the crystalline and amorphous phases, respectively. One

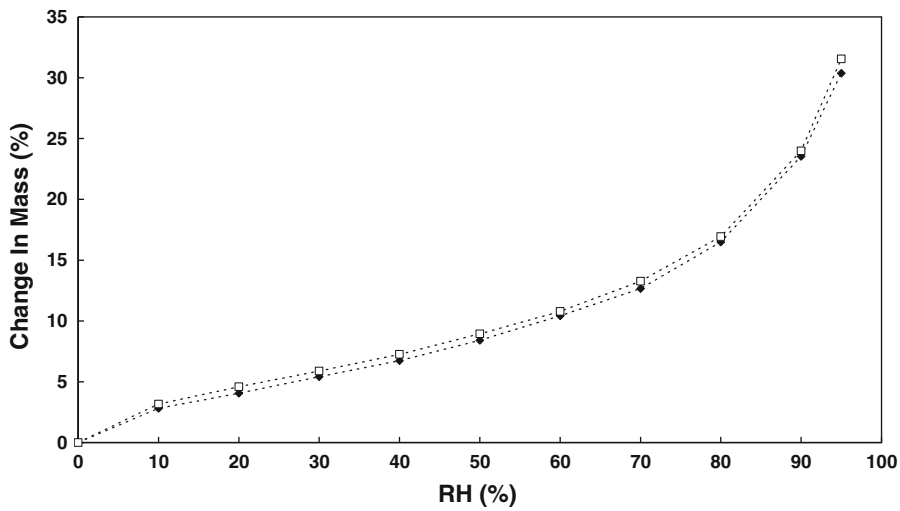

Fig. 5 Water sorption isotherm for a MFC film prepared from a dispersion homogenized 10 times. The thicknesses of the films are 5.1 μm

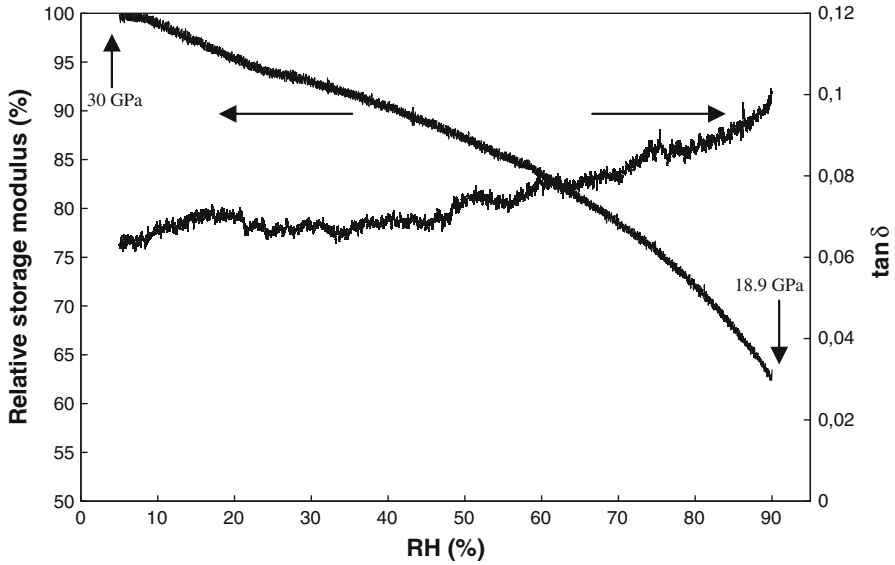

Fig. 6 DMA of a MFC film prepared by from a dispersion homogenized 10 times. The thickness of the film is 5.1 μm. The width of the sample was 3 mm and the clamping distance was 9 mm

obtains a value of ≈ 48 GPa for E_A from Eqs. 1 and 2, using values of 90 and 220 GPa for the highly oriented and crystalline fiber, respectively. This result is in large agreement with a previous study by Jeronimidis et al. (Jeronimidis and Vincent 1984) where the elastic modulus for amorphous cellulose was measured to 50 GPa.

Using sorption isotherms for the MFC film, RH was converted into moisture content (Fig. 7). OTR is non-linearly dependent on the moisture content, and a sharp increase in OTR was observed above a moisture content of 15%. The effect of moisture on OTR is most probably governed by the content of plasticizing water in the film, depending on the structure of the film, which is rigid and vitreous at low moisture contents and rubbery and viscous at high moisture contents.

Surface structure and air permeability properties of MFC coated papers

The air permeability is shown in Fig. 8 as a function of the coat weight of MFC for the coated papers. At zero MFC coverage or coat weight i.e. for the pure unbleached and greaseproof papers, the air permeability was 69,000 and 660 nm/Pa s, respectively. When a thin coat was applied on the two papers,

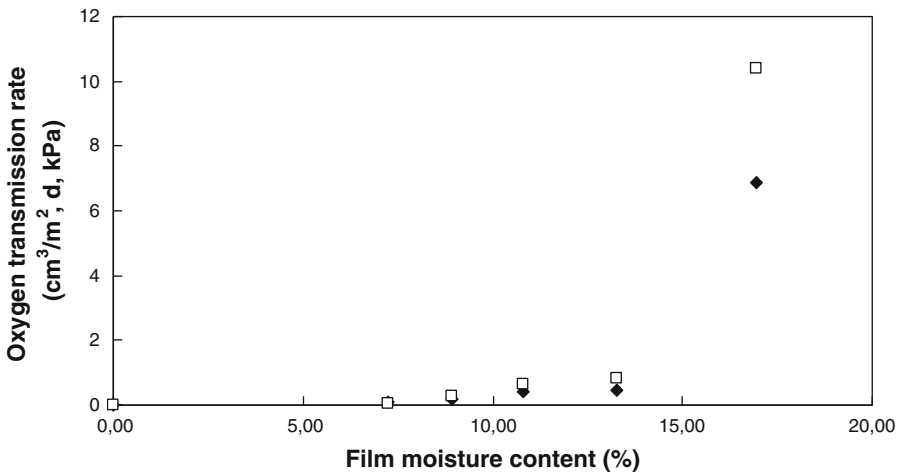

Fig. 7 Effect of film moisture content on oxygen transmission rates (OTR) of MFC films prepared from dispersions homogenized once (*open square*) and ten times (*filled diamond*), respectively. The thicknesses of the films are 5.1 μm

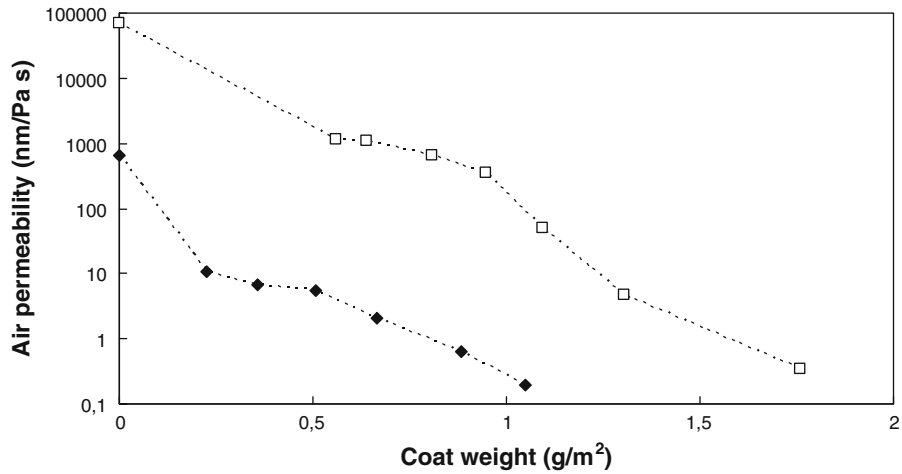

Fig. 8 Air permeability (logarithmic scale) as a function of MFC-coat weight for an unbleached (*open square*) and a greaseproof paper (*filled diamond*) coated on a bench scale. The unbleached paper was coated twice using the largest wire diameter rod to ensure a complete surface coverage of MFC. The air permeability was then 0.3 nm/Pa s. The average coefficient of variations was 4.51 and 3.19% for the determination of coat weights and air permeability, respectively

the air permeability decreased drastically. For the unbleached and greaseproof paper coated using the largest wire diameter rod, the air permeability was 4.8 and 0.2 nm/Pa s, respectively. The unbleached paper was coated twice using the largest wire diameter rod to ensure a complete surface coverage of MFC. The air permeability was then 0.3 nm/Pa s. The coat weight on the unbleached paper was higher then that on greaseproof paper, especially at low levels of coating. The highest coat weights obtained in a single coating step were ca. 1.3 and 1.0 g/m^2 for the unbleached and greaseproof paper, respectively.

The surface structures of the MFC-coated and uncoated unbleached and greaseproof papers were studied using E-SEM. The results of this study are summarized in Figs. 9 and 10, which show micrographs of the papers with different coat weights. The unbleached paper (Fig. 9a) shows a very open and porous network of randomly crossed fibers. When the coating weight was increased slightly (Fig. 9b), the network structure of the paper became less apparent. A further increase in the MFC-coat weight led to film formation of the coating layer (Fig. 9c), and eventually, when the paper was coated twice (Fig. 9d), to a hardly visible fibre structure in the base paper. The micrograph shows that the coating had covered the fibers at that coat weight and that the coating formed a continuous film over the fibers. As expected, the greaseproof paper (Fig. 10a) revealed a closer and less porous structure than the unbleached paper. As the unbleached paper, when the coat weight on the greaseproof paper increased slightly (Fig. 10b), the network structure became less apparent and a continuous MFC film was formed. When the same coat weight of MFC was applied on both base substrates, the greaseproof paper exhibited a more dense structure, which correlates well with the air permeability measurements in Fig. 8.

Oil resistance

Figure 11 shows the oil resistance of the coated unbleached and greaseproof paper as a function of the air permeability. The penetration times of castor oil and turpentine oil are shown. When the air permeability decreased, i.e., increased coat weight, the oil resistance increased. It is evident that the coated paper with the lowest air permeability, <1 nm/Pa s, exhibited superior oil resistance (>1,800 s for castor oil), and that there was great difference in penetration time between the two oils. The oil penetrated the unbleached paper immediately (1 s). The coated greaseproof paper is more resistant towards the oil since it exhibited lower air permeability.

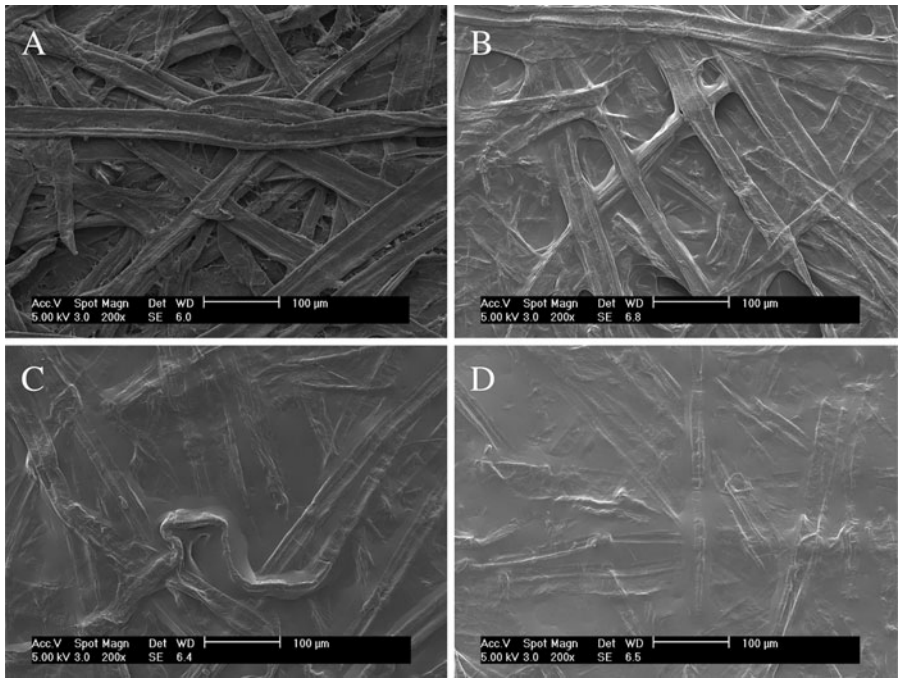

Fig. 9 E-SEM micrographs of uncoated (**a**) and MFC-coated unbleached papers with coat weights of ca. 0.9 (**b**), 1.3 (**c**) and 1.8 g/m^2 (**d**), respectively. The *scale bar* is 100 µm

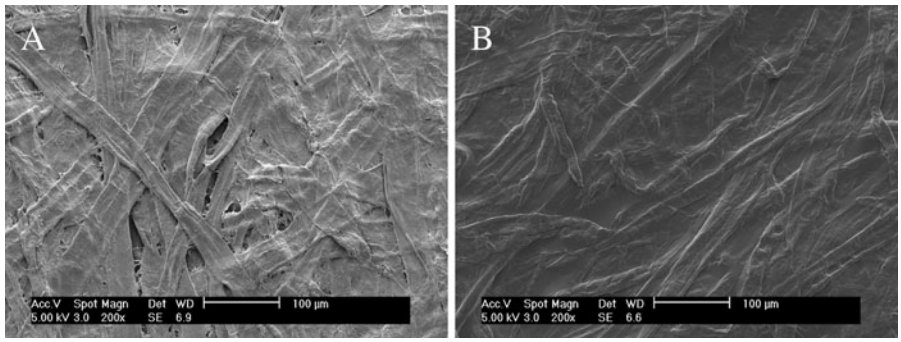

Fig. 10 E-SEM micrographs of uncoated (**a**) and MFC-coated (**b**) greaseproof papers with a coat weight of ca. 0.7 g/m^2. The *scale bar* is 100 µm

Discussion

Influence of microstructure and water adsorption on oxygen permeability

As shown in Fig. 4a, an increase in MFC coating thickness/grammage resulted in a dramatic reduction in the OTR value. This simply indicates an increase in the tortuous path of oxygen and an enhancement of the barrier properties. Since the OP of the films decreased with increasing film thickness, it is believed that most pores are located at the surface of the MFC films and that these pores are not connected, thus contributing to the impermeable nature of the films.

A number of examples in the literature demonstrate the relationship between crystallinity and permeability, where a higher crystallinity is associated with a lower permeability (McGonigle et al. 2000). The crystalline regions of a polymer film are non-permeable and this increases the path-length of diffusing

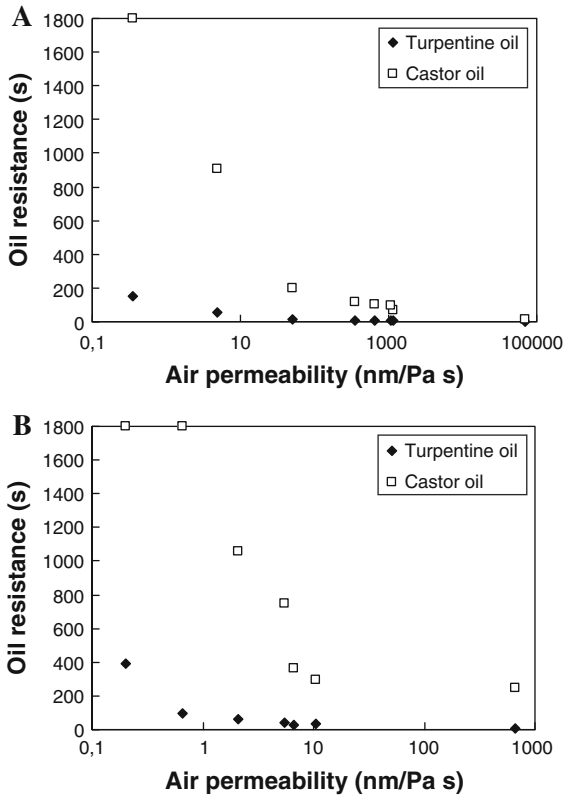

Fig. 11 Oil absorption according to Tappi T-454 as a function of air permeability for (**a**) unbleached and (**b**) greaseproof paper coated with MFC. Results for both castor oil (*open square*) and turpentine oil (*filled diamond*) are included in the figure. The maximum oil resistance value in the test is 1,800 s. The average coefficient of variations for the oil absorption was 20.8 and 19.1% for the unbleached and greaseproof paper, respectively

permeant. Since MFC fibrils exhibit a degree of crystallinity of 63 ± 8.6%, (Aulin et al. 2009) it is expected that the polymer chain mobility should be rather low, thus contributing to the very low OTR-values at 0% RH. MFC exhibits a complex ability to form inter- and intra-hydrogen bonds between the hydroxyl groups (-OH) of fibrils and the cellulose chains of the individual microfibrils, respectively. Many studies have shown that intermolecular interactions (mostly H-bonding and van der Waals interactions) lead to a more compact packing and higher cohesive energy density and lower free-volumes associated with lower gas permeability (Fried et al. 1978; Pedrosa et al. 1994; Labuschagne et al. 2008). The presence of impermeable crystalline regions together with the denser amorphous region leads to greater gas barrier properties and could partly explain the very low OTR-values obtained. To distinguish in greater detail between the effects of the degree of crystallinity, the cohesive energy density and the free volume on the permeability, a systematic investigation by a combination of dynamic mechanical analysis, small-angle X-ray scattering and positronium lifetime measurement may be considered (Ito et al. 2001).

The MFC films were also studied at various relative humidities, and the OTR was found to increase substantially with increasing RH (Fig. 4b). At a RH higher than 70%, the curve showed a sharp increase in OTR for the highest RH levels. Such behavior is typical of hydrophilic polymers including cellophane, ethylene polyvinyl alcohol or methylcellulose/palmitic acid films. This effect of high RH on OTR was previously observed for other edible film types (Gontard et al. 1992; McHugh and Krochta 1994a, b, c; Gontard et al. 1996) and could be linked to a sharp increase in polymeric chain mobility. The observed increase in the OTR in the 40–80% RH range might be related to the plasticization effect of the amorphous MFC domains by sorbed water molecules, as shown by the DVS and DMA measurements. Water molecules sorbed to the surface or in the amorphous zones of the fibrils may disrupt hydrogen bonding and weakening the fibril/fibril joint formation, resulting in an increased mobility of the fibril network. This creates additional sites for the permeation of oxygen and increased mobility of oxygen molecules within the polymer network. In addition to an increased permeability due to structural modifications of the fibril network, an increase in oxygen solubility by increased moisture content in the film is expected. The permeability coefficient is commonly known as the product of diffusivity and solubility and oxygen solubility has been previously studied for wheat gluten (Gontard et al. 1996) and starch based (Dole et al. 2004) films with a high moisture content.

Apart from the influence of crystallinity, and the ability of the MFC network to form hydrogen bonds, the microstructure of the MFC films is believed to play a significant role for the oxygen permeability properties. The OTR values seem to decrease with increasing in film thickness, supporting the pore blocking theory, i.e., less connected pores throughout the film. A dense film structure is indicated by the density measurements. The density is assumed to be higher in the bulk than at the surface of the film, and

this may result in more porous and permeable surface layers than those of the interior. Dense microstructures and very large fractions of microfibrils with a width of ca. 5–10 nm are also indicated by the micrographs of the films. It is believed that the large fractions of nanofibers contribute to the impermeable nature of the films and the large similarities in the OTR values obtained from the films prepared from dispersions homogenized at different levels. Table 2 shows the OP of MFC films compared with literature values for various bio-based and synthetic polymers. At 0% RH, MFC films presented very low oxygen permeability values compared to other edible, biodegradable or synthetic films. For example, the oxygen permeability of MFC films at 0% RH was in the same range as that of poly(vinylalcohol), 10,000-times lower than that of polyethylene and 20,000-times lower than that of polystyrene. The measured oxygen permeability at 50% RH was lower than the literature values for glycerol-plasticized starch, whey protein and arabinoxylan and comparable to the often used barrier plastic ethylene vinyl alcohol (EVOH), see Table 2. The measured oxygen permeability was lower than literature values for other types of MFC (Syverud and Stenius 2009). This is probably due to the carboxymethylation pretreatment used in the

Table 2 Oxygen permeability data for MFC films and literature values for some renewable and synthetic polymers

Material	Oxygen permeability (cm^3 μm)/(m^2 day kPa)	Source and conditions
MFC (carboxymethylated)	0.0006	Present study, 0% RH
MFC (carboxymethylated)	0.85	Present study, 50% RH
MFC (not pre-treated)	3.52–5.03	(Syverud and Stenius 2009),50% RH
TEMPO-oxidized nanocellulose	0.004	(Fukuzumi et al. 2009), 0% RH
O-acetylgalactoglucomannan	2.0	(Hartman et al. 2006a, b), 50% RH
O-acetylgalactoglucomannan-alginate (7:3)	0.55	(Hartman et al. 2006a, b), 50% RH
O-acetylgalactoglucomannan-CMC (7:3)	1.28	(Hartman et al. 2006a, b), 50% RH
Whey protein–glycerol (3:1–0.8:1)	40-330	(Sothornvit and Krochta 2000), 50% RH
Whey protein–sorbitol (1.5:1)	1.03	(McHugh and Krochta 1994a, b, c), 30% RH
Amylose–glycerol (2.5:1)	7	(Rindlav-Westling et al. 1998), 50% RH
Amylopectin–glycerol (2.5:1)	14	(Rindlav-Westling et al. 1998), 50% RH
Cellophane	0.41	(Wu and Yuan 2002),0% RH
Cellophane–glycerol	9.5	(Newton and Rigg 1979), 50% RH
Chitosan–glycerol (4:1)	0.01–0.04	(Butler et al. 1996), 0% RH
Chitosan–glycerol (2:1)	0.04–0.08	(Butler et al. 1996), 0% RH
65% Glucuronoxylan/35% xylitol	0.21	(Gröndahl et al. 2004), 50% RH
Arabinoxylan	2	(Höije et al. 2008), 50% RH
Collagen	1.2	(McHugh and Krochta 1994a, b, c), 0% RH
Microcrystalline wax	1,540	(McHugh and Krochta 1994a, b, c), 0% RH
Carnauba wax	157	(McHugh and Krochta 1994a, b, c), 0% RH
Polyvinylidene chloride (PVDC)	0.1–3	(Lange and Wyser 2003), 50% RH
Polyvinylalcohol (PVOH)	0.20	(Lange and Wyser 2003), 0% RH
Polyamide (PA)	1–10	(Lange and Wyser 2003), 0% RH
Poly(ethylene-terephthalate) PET	10–50	(Lange and Wyser 2003), 50% RH
Poly(vinyl chloride) PVC	20–80	(Lange and Wyser 2003), 50% RH
Poly(lactic acid) (PLA)	184	(Fukuzumi et al. 2009), 0% RH
Polypropylene (PP)	494–987	(Lange and Wyser 2003), 50% RH
Polystyrene (PS)	987–1,481	(Lange and Wyser 2003), 50% RH
Low-density polyethylene (LDPE)	1,900	(McHugh and Krochta 1994a, b, c), 50% RH
Ethylene vinyl alcohol (EVOH)	0.01–0.1	(Lange and Wyser 2003), 0% RH

present study, which makes the fibrils highly charged and easier to liberate, and thus gives smaller and more uniform fibril dimensions (5–10 nm) than in untreated low-charged MFC (Syverud and Stenius 2009), where the fibril width was considerably thicker.

Influence of coating layer properties on the air permeability

The very low air permeability of the coated papers suggests that there are very few connected pores through the cross section of the coated paper and that a partly crystalline MFC layer may form on the paper surface. Similar conclusions were drawn by Syverud et al. (Syverud and Stenius 2009), who studied the barrier properties of MFC-coated sheets. Although it should be stressed that the authors used non-pre-treated MFC and a coating process with the aid of a dynamic sheet former. Further, it is believed that a crystalline layer in contact with the cellulose fibers will constitute an obstacle for the transport of penetrates such as turpentine and castor oil through the system and cause an extension of the diffusion path. Maximum coat weights obtained for single coatings on the unbleached and greaseproof papers were ca 1.3 and 1.1 g/m^2, respectively. Higher coat weighs could not be achieved using a MFC dispersion of 0.85 wt% in the coating with a laboratory-scale rod coater. The concentration of the dispersion must be considerably higher if a higher coat weight is to be obtained. An alternative coating technique which yields higher coat weights may also be needed. Curtain or extrusion coating may offer that possibility (Kjellgren et al. 2006). The air permeability values obtained are very low compared to what has been reported previously in the literature and is fully comparable to greaseproof paper produced from highly refined sulfite/sulfate pulp (Kjellgren and Engström 2006). MFC coat weights of ca. 1.8 and 1.1 g/m^2 for the unbleached and greaseproof papers, respectively, resulted in air permeability's as low as $<$1 nm/Pa s. For comparison, it can be mentioned that Kjellgren et al. (Kjellgren and Engström 2006) have reported air permeability values of 24,000 and 1.7 nm/Pa s, respectively, for the same unbleached and greaseproof papers coated with 3.4 g/m^2 of chitosan. The air permeability of the coated material had a great influence on the oil resistance. The air permeability measurements and the oil resistance test showed that MFC can be used as a coating on both wrapping paper and greaseproof paper to obtain a material with oil barrier properties, provided that the coating seals the pores in the base paper and forms a continuous and homogeneous film.

Conclusions

MFC produced from dissolving pulp can be used to prepare transparent free films and to coat thin layers on base papers. FE-SEM micrographs showed that the MFC films consisted of randomly assembled nano-fibers, mostly with a thickness of ca. 5–10 nm, although some larger entities were found. The OP of the free film was evaluated, and it was found that the films possessed very low OP-values at low RH (0%), although the oxygen transmission rate increased with increasing RH. The storage modulus of the films decreased when the surrounding RH was increased in a humidity scan in DMA. The dense structure formed by the semi-crystalline microfibrils and their ability to form intra- and inter-fibrillar hydrogen bonds are believed to contribute to the superior barrier properties of the films. The oxygen permeability was lower than, for example, that of plasticized starch, whey protein and arabinoxylan and in the same range as that of commercially used synthetic polymeric material EVOH. The air permeability of the coated paper decreased considerably with an MFC coating. The reduced surface porosity induced by fibrils, as studied by E-SEM, explains the superior oil barrier properties. In summary, the MFC films and coatings are promising for potential applications as transparent and biodegradable packaging films with high barrier properties.

Acknowledgments The authors wish to thank BIM Kemi Sweden AB and the Knowledge Foundation through its graduate school YPK for financial support. Professor Lars Ödberg, Dr. Torbjörn Pettersson and Dr. Henrik Kjellgren are acknowledged for valuable discussions. Joanna Hornatowska is gratefully acknowledged for help with the E-SEM measurements.

References

Arvanitoyannis IS (2006) Handbook of biodegradable polymeric materials and their applications. American Scientific Publishers, US

Arvanitoyannis I, Psomiadou E, Nakayama A, Aiba S, Yamamoto N (1997) Edible films made from gelatin, soluble starch and polyols, part 3. Food Chem 60:593–604

Arvanitoyannis I, Nakayama A, Aiba S-I (1998) Edible films made from hydroxypropyl starch and gelatin and plasticized by polyols and water. Carbohydr Polym 36:105–119

Asthana SK, Koteswara Rao MVR, Balakrishna KJ (1964) Pinene-free turpentine as a paint thinner. Perfumery Essential Oil Record 55:725–727

Aulin C, Ahola S, Josefsson P, Nishino T, Hirose Y, Österberg M, Wågberg L (2009) Nanoscale cellulose films with different crystallinities and mesostructures-their surface properties and interaction with water. Langmuir 25:7675–7685

Avranitoyannis I, Psomiadou E, Nakayama A (1997) Edible films made from sodium caseinate, starches, sugars or glycerol. Part 1. Carbohydr Polym 31:179–192

Bardage S, Donaldson L, Tokoh C, Daniel G (2004) Ultrastructure of the cell wall of unbeaten Norway spruce pulp fibre surfaces. Nordic Pulp Paper Res J 19:448–452

Bercea M, Navard P (2000) Shear dynamics of aqueous suspensions of cellulose whiskers. Macromolecules 33: 6011–6016

Butler BL, Vergano PJ, Testin RF, Bunn JM, Wiles JL (1996) Mechanical and barrier properties of edible chitosan films as affected by composition and storage. J Food Sci 61:953–955, 961

Chanzy H (2009) Personal communication

Chen W, Lickfield GC, Yang CQ (2004) Molecular modeling of cellulose in amorphous state part II: effects of rigid and flexible crosslinks on cellulose. Polymer 45:7357–7365

Cox HL (1952) The elasticity and strength of paper and other fibrous materials. Br J Appl Physics 3:72–79

Deisenroth E, Jho C, Haniff M, Jennings J (1998) The designing of a new grease repellent fluorochemical for the paper industry. Surf Coatings Int 81:440–447

Diddens I, Murphy B, Krisch M, Mueller M (2008) Anisotropic elastic properties of cellulose measured using inelastic X-ray scattering. Macromolecules 41:9755–9759

Dole P, Joly C, Espuche E, Alric I, Gontard N (2004) Gas transport properties of starch based films. Carbohydr Polym 58:335–343

Ebeling T, Paillet M, Borsali R, Diat O, Dufresne A, Cavaille JY, Chanzy H (1999) Shear-induced orientation phenomena in suspensions of cellulose microcrystals, revealed by small angle X-ray scattering. Langmuir 15:6123–6126

Fengel D (1971) Ultrastructural organization of the cell wall components. J Polym Sci, Polym Symposia 36:383–392

Fried JR, Karasz FE, MacKnight WJ (1978) Compatibility of poly(2, 6-dimethyl-1, 4-phenylene oxide) (PPO)/poly(styrene-co-4-chlorostyrene) blends. 1. Differential scanning calorimetry and density studies. Macromolecules 11: 150–158

Fukuzumi H, Saito T, Iwata T, Kumamoto Y, Isogai A (2009) Transparent and high gas barrier films of cellulose nanofibers prepared by TEMPO-mediated oxidation. Biomacromolecules 10:162–165

Gontard N, Guilbert S, Cuq JL (1992) Edible wheat gluten films: influence of the main process variables on film properties using response surface methodology. J Food Sci 57:190–195, 199

Gontard N, Thibault R, Cuq B, Guilbert S (1996) Influence of relative humidity and film composition on oxygen and carbon dioxide permeability's of edible films. J Agric Food Chem 44:1064–1069

Gröndahl M, Eriksson L, Gatenholm P (2004) Material properties of plasticized hardwood xylans for potential application as oxygen barrier films. Biomacromolecules 5:1528–1535

Hansen NML, Plackett D (2008) Sustainable films and coatings from hemicelluloses: a review. Biomacromolecules 9:1493–1505

Hartman J, Albertsson A-C, Lindblad MS, Sjöberg J (2006a) Oxygen barrier materials from renewable sources: material properties of softwood hemicellulose-based films. J Appl Polym Sci 100:2985–2991

Hartman J, Albertsson A-C, Sjöberg J (2006b) Surface- and bulk-modified galactoglucomannan hemicellulose films and film laminates for versatile oxygen barriers. Biomacromolecules 7:1983–1989

Henriksson M, Berglund LA, Isaksson P, Lindström T, Nishino T (2008) Cellulose nanopaper structures of high toughness. Biomacromolecules 9:1579–1585

Herrick FW, Casebier RL, Hamilton JK, Sandberg KR (1983) Microfibrillated cellulose: morphology and accessibility. JAppl Polym Sci: Appl Polym Symp 37:797–813

Höije A, Sternemalm E, Heikkinen S, Tenkanen M, Gatenholm P (2008) Material properties of films from enzymatically tailored arabinoxylans. Biomacromolecules 9:2042–2047

Ito K, Saito Y, Yamamoto T, Ujihira Y, Nomura K (2001) Correlation study between oxygen permeability and free volume of ethylene-vinyl alcohol copolymer through positronium lifetime measurement. Macromolecules 34: 6153–6155

Jeronimidis G, Vincent JFV (1984) Composite materials. Topics Mol Struct Biol 5:187–210

Kendall K (2001) Molecular adhesion and its applications: the sticky universe. Kluwer Academic/Plenum Publishers, New York

Kissa E (2001) Fluorinated surfactants and repellents, revised and expanded. Marcel Dekker, New York

Kjellgren H, Engström G (2006) Influence of base paper on the barrier properties of chitosan-coated papers. Nordic Pulp Paper Res J 21:685–689

Kjellgren H, Gällstedt M, Engström G, Järnström L (2006) Barrier and surface properties of chitosan-coated greaseproof paper. Carbohydr Polym 65:453–460

Kohler R, Alex R, Brielmann R, Ausperger B (2006) A new kinetic model for water sorption isotherms of cellulosic materials. Macromol Symp 244:89–96

Krochta JM (2007) Food packaging. Marcel Dekker Inc, New York

Labuschagne PW, Germishuizen WA, Verryn SMC, Moolman FS (2008) Improved oxygen barrier performance of poly(vinyl alcohol) films through hydrogen bond complex with poly(methyl vinyl ether-co-maleic acid). Eur Polym J 44:2146–2152

Lange J, Wyser Y (2003) Recent innovations in barrier technologies for plastic packaging—a review. Packaging Technol Sci 16:149–158

McGonigle EA, Liggat JJ, Pethrick RA, Jenkins SD, Daly JH, Hayward D (2000) Permeability of N2, Ar, He, O2 and CO2 through biaxially oriented polyester films—dependence on free volume. Polymer 42:2413–2426

McHugh TH, Krochta JM (1994a) Edible coatings films improve food quality. Technomic, Lancaster

McHugh TH, Krochta JM (1994b) Permeability properties of edible films. CRC Press, US

McHugh TH, Krochta JM (1994c) Sorbitol- vs glycerol-plasticized whey protein edible films: integrated oxygen permeability and tensile property evaluation. J Agric Food Chem 42:841–845

Miller KS, Krochta JM (1997) Oxygen and aroma barrier properties of edible films: a review. Trends Food Sci Technol 8:228–237

Newton KG, Rigg WJ (1979) The effect of film permeability on the storage life and microbiology of vacuum-packed meat. J Appl Bacteriol 47:433–441

Ono H, Yamada H, Matsuda S, Okajima K, Kawamoto T, Iijima H (1998) Proton-NMR relaxation of water molecules in the aqueous microcrystalline cellulose suspension systems and their viscosity. Cellulose 5:231–247

Orts WJ, Godbout L, Marchessault RH, Revol JF (1998) Enhanced ordering of liquid crystalline suspensions of cellulose microfibrils: a small-angle neutron scattering study. Macromolecules 31:5717–5725

Pääkkö M, Ankerfors M, Kosonen H, Nykänen A, Ahola S, Österberg M, Ruokolainen J, Laine J, Larsson PT, Ikkala O, Lindström T (2007) Enzymatic hydrolysis combined with mechanical shearing and high-pressure homogenization for nanoscale cellulose fibrils and strong gels. Biomacromolecules 8:1934–1941

Pedrosa P, Pomposo JA, Calahorra E, Cortazar M (1994) On the glass transition behavior, interaction energies, and hydrogen-bonding strengths of binary poly(p-vinylphenol)/polyether blends. Macromolecules 27:102–109

Psomiadou E, Arvanitoyannis I, Yamamoto N (1997) Edible films made from natural resources; microcrystalline cellulose (MCC), methylcellulose (MC) and corn starch and polyols. Part 2. Carbohydr Polym 31:193–204

Rindlav-Westling A, Stading M, Hermansson A-M, Gatenholm P (1998) Structure, mechanical and barrier properties of amylose and amylopectin films. Carbohydr Polym 36: 217–224

Schwartz C (1981) Oil resistance utilizing fluorochemicals. Technical association of the pulp and paper industry, section sizing, Chicago. Tappi Press, US

Sothornvit R, Krochta JM (2000) Plasticizer effect on oxygen permeability of beta -lactoglobulin films. J Agric Food Chem 48:6298–6302

Svagan AJ, Samir MASA, Berglund LA (2007) Biomimetic polysaccharide nanocomposites of high cellulose content and high toughness. Biomacromolecules 8:2556–2563

Syverud K, Stenius P (2009) Strength and barrier properties of MFC films. Cellulose 16:75–85

Turbak AF, Snyder FW, Sandberg KR (1983) Microfibrillated cellulose, a new cellulose product: properties, uses, and commercial potential. J Appl Polym Sci: Appl Polym Symp 37:815–827

Wågberg L, Winter L, Ödberg L, Lindström T (1987) On the charge stoichiometry upon adsorption of a cationic polyelectrolyte on cellulosic materials. Colloids Surf 27:163–173

Wågberg L, Decher G, Norgren M, Lindström T, Ankerfors M, Axnäs K (2008) The build-up of polyelectrolyte multilayers of microfibrillated cellulose and cationic polyelectrolytes. Langmuir 24:784–795

Winter L, Wågberg L, Ödberg L, Lindström T (1986) Polyelectrolytes adsorbed on the surface of cellulosic materials. J Colloid Interf Sci 111:537–543

Wu J, Yuan Q (2002) Gas permeability of a novel cellulose membrane. J Membr Sci 204:185–194

Yano H, Sugiyama J, Nakagaito AN, Nogi M, Matsuura T, Hikita M, Handa K (2005) Optically transparent composites reinforced with networks of bacterial nanofibers. Adv Mater 17:153–155